Journal of ELECTRONIC MATERIALS, Vol. 33, No. 12, 2004 *Special Issue Paper*

Effect of Cu Concentration on Morphology of Sn-Ag-Cu Solders by Mechanical Alloying

SZU-TSUNG KAO[1] and JENQ-GONG DUH[1,2]

1.—Department of Materials Science and Engineering, National Tsing Hua University, Hsinchu, Taiwan. 2.—E-mail: jgd@mx.nthu.edu.tw

The mechanical alloying (MA) process is considered an alternative approach to produce solder materials. In this study, the effect of Cu concentration in the ternary Sn-3.5Ag-xCu (x = 0.2, 0.7, and 1) solder by MA was investigated. The (Cu,Sn) solid solution was precipitated as the Cu_6Sn_5 intermetallic compound (IMC), which was distributed nonuniformly through the microstructure. The Cu_6Sn_5 IMC, which was present in the SnAgCu solder with high Cu composition, causes the as-milled MA particle to fracture to a smaller size. Appreciable distinction on morphology of as-milled MA powders with different Cu content was revealed. When the Cu concentration was low (x = 0.2), MA particle aggregated to a spherical ingot with large particle size. For higher Cu concentration (x = 0.7 and x = 1), the MA particle turned to flakes with smaller particle size. The distinction of the milling mechanism of Sn-3.5Ag-xCu (x = 0.2, 0.7, and 1) solder by the MA process was discussed. An effective approach was developed to reduce the particle size of the SnAgCu solder from 1 mm down to 10–100 μm by doping the Cu_6Sn_5 nanoparticle during the MA process. In addition, the differential scanning calorimetry (DSC) results also ensure the compatibility to apply the solder material for the reflow process.

Key words: Mechanical alloying (MA), lead-free solder paste, welding, fracturing, composite solder

INTRODUCTION

Electronic packaging is a technology of manufacturing electronic products that are composed of integrated circuits chips and electric devices.[1,2] Because solder provides the electrical and mechanical connection between the silicon die and the bonding pad, the material selections for solder alloys are very critical. The SnPb-based solder alloys are the most used materials in the electronic industry for many advantages, such as low cost, high ductility, low surface tension, and low eutectic temperature.[1] However, with the concern of human health and nature environment, the investigation of an alternative Pb-free solder is necessary.[3–15] A large number of Pb-free solder alloys have been proposed, such as Sn-Ag, Sn-Bi, Sn-Ag-Bi, and Sn-Ag-Cu.[3–23] The Sn-Ag-Cu system has low eutectic temperature, slow growth rate of the intermetallic layer at the interface, high strength, and a low wetting angle.[12–15] Therefore, Sn-Ag-Cu solder alloys are the most promising candidates among Pb-free solder materials. A recent study reported that the reactions between under-bump metallization and Sn-Ag-Cu solders depended strongly on the Cu concentration of the solders.[24] Therefore, the controllability and the facility to produce solder materials with specific compositions is essential.

There are many methods to produce solder alloys, and the mechanical alloying (MA) technique is one of them. The characteristics of the MA process have been studied in the literature.[25–28] It is a solid-state process technique to produce particles with submicron homogeneity by repeated welding, fracturing, and rewelding powder particles in a high-energy ball mill.[31] It overcomes the disadvantage of forming new alloys by using a starting mixture of low- and high-melting temperature elements. Precise control over the solder composition is also an advantage of the MA technique.

(Received April 1, 2004; accepted June 25, 2004)

In addition, it is a convenient method to produce commercial solder pastes by adding flux directly to MA powders. Recently, Lai and Duh showed SnAg and SnAgBi solder materials by the MA technique,[28] in which good wettability and good alloying performance were revealed.

The purpose of this study was to develop an alternative approach to derive the SnAgCu lead-free solder by the MA process. It was aimed to effectively decrease the particle size to less than 100 μm. The effect of Cu composition on the morphology of the SnAgCu MA powder was investigated. Besides the thermal behavior of SnAgCu powders, the MA process was also evaluated to ensure its process compatibility during reflow.

EXPERIMENTAL PROCEDURE

To compare the influence of Cu content on the morphology of SnAgCu solder powder, the total weight of the input powder was fixed to 5 g, while the amount of Cu was varied from 0.2 wt% to 1 wt%. Powders of Sn (−100 mesh, purity 99.85 wt.%, Alfa Aesar, Ward Hill, MA), Ag (5–8 μm, 99.9 wt.%, Aldrich Chemical Co., Milwaukee, WI), and Cu (10 μm, 99.9wt.%, Alfa Aesar) were used as starting materials in this study. Alcohol was added into powders as the surfactant to reduce excessive cold welding. Mechanical alloying was performed at room temperature in a high-energy planetary ball mill (Pulverisette 5, Fritsch, Germany). A zirconia container and milling balls of both 1 cm and 3 mm in diameter were used. The ball-to-powder weight ratio was maintained at 26:1. The rotation speed was fixed at 150 rpm. To ensure the homogeneity, the compositions of the MA powder were analyzed with an inductively coupled plasma-atomic emission spectrometer (ICP-AES, Optima 3000 DV, Perkin Elmer, Eden Prairie, MN). The powders were also compacted and polished for electron probe microanalyzer (EPMA) examination.

The crystal structure of MA powders was identified with an x-ray diffractometer (D/MAX-B, Rigaku, Tokyo) using a wavelength of Cu K_α ($\lambda = 1.5406$ Å). A differential scanning calorimetry (DSC) tester (6200, Seiko, Tokyo) was used to measure the melting point of as-fabricated solder powders. During the test, MA powders were heated at the rate of 10°C/min under a N_2 atmosphere.

Nanoscale Cu_6Sn_5 powders were synthesized by a chemical method, which involved reducing a solution of $Cu(NO_3)_2$ and $Sn(SO)_4$.[29] Twice the amount of the $NaBH_4$ solution was added to the solution containing the Cu and Sn ions to ensure complete reduction of the metal ions. Upon addition of the $NaBH_4$ solution, a black precipitate was immediately observed. The black precipitate was washed with distilled water and then dried at room temperature. The particle size, shape, and morphology of as-milled MA powders were observed with field-emission scanning electron microscopy (FESEM, JSM-6500F, JEOL, Tokyo).

Table I. ICP-AES Results of Sn3.5AgxCu Solder Powders Milled for 70 h by the MA Process

Nominal Cu Concentration in Synthesis	ICP-AES Measured Cu Concentration (wt.%)
0.2	0.187
0.7	0.699
1.0	1.010

RESULTS AND DISCUSSION

Characteristics of MA Powders and Milling Mechanisms

The Cu concentrations analyzed by ICP-AES from the SnAgCu solder alloy produced by MA process are listed in Table I. The ICP-AES derived concentration of the as-fabricated solder powders by the MA process was fairly close to the nominal one. To ensure accurate measurement, each powder composition was measured by ICP several times, and the average results were obtained. The detailed composition of compacted powders was also measured by EPMA, as illustrated in Fig. 1. The result of the Cu composition from EPMA was also in agreement with the nominal composition of 0.2 wt.%. In fact, the accurate control of Cu content in solders was essential. The intermetallic compound (IMC) formed between the solder and the under-bump metallization layer was sensitive to the Cu content in the SnAgCu solder.[24] Therefore, the MA process provided the controllability and the facility to fabricate the SnAgCu solder alloy.

Figure 2 shows the SEM micrographs of Sn, Ag, and Cu raw powders. The size of the input powder was around 5–25 μm. Through MA, raw particles were repeatedly flattened, cold-welded, fractured, and rewelded to form Sn-Ag-Cu solder powders, as shown in Fig. 3a. The powders revealed different morphologies after various milling time. After 10-h milling, the powders were pressed to thin and flat plates, which were around 200 μm in size. The plates were flattened to much thinner in thickness

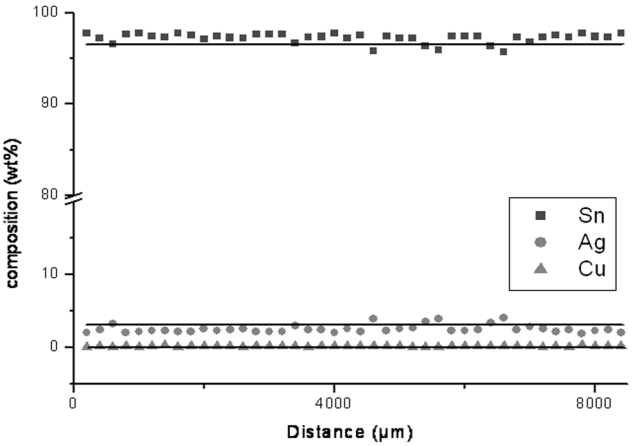

Fig. 1. Homogeneity of Sn-3.5Ag-0.2Cu powders milled for 70 h (probe size: 200 μm).

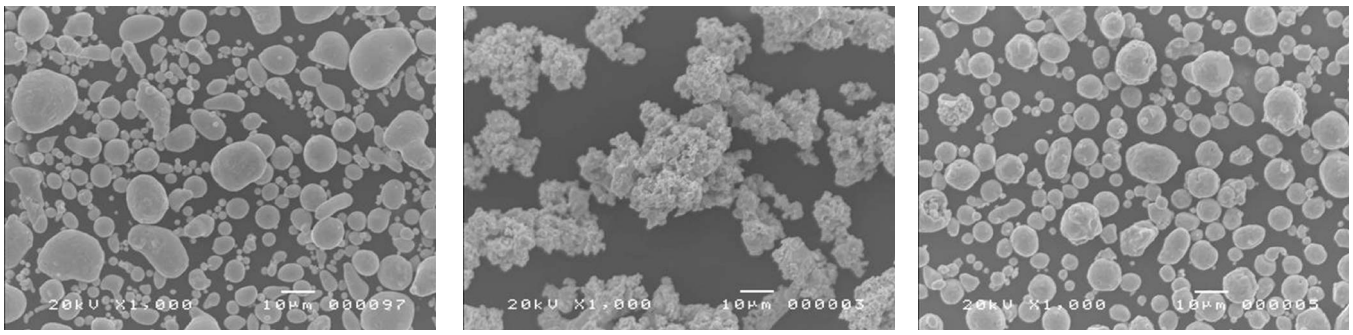

Fig. 2. The SEI micrographs of Sn, Ag, and Cu raw powders.

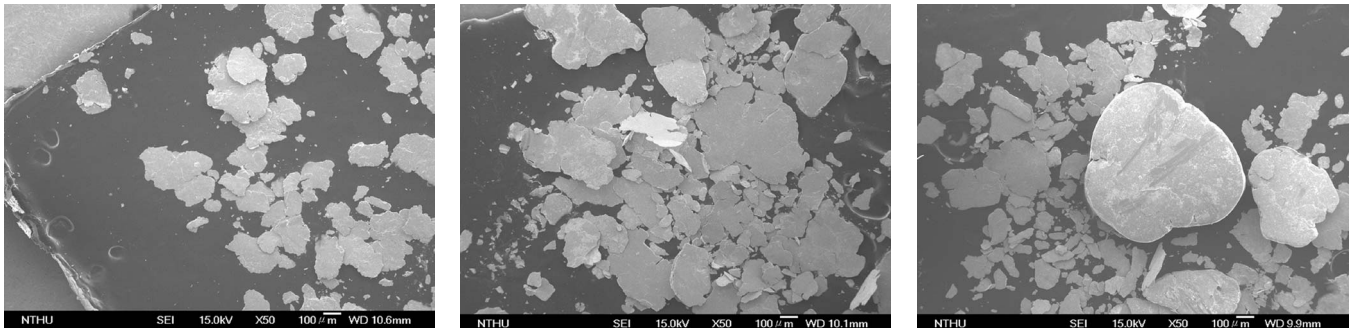

a b c

Fig. 3. The SEI micrographs of the Sn-3.5Ag-0.2Cu MA powders milled for (a) 10 h, (b) 55 h, and (c) 90 h.

and larger in cross-sectional area after milling for 55 h (Fig. 3b). With longer milling time up to 90 h, the plates were cold-welded together and piled up to form a large ingot with a diameter of 1 mm (Fig. 3c).

The milling mechanism might be explained from the morphology evolution. Because the raw material, i.e., Sn, Ag, and Cu powders, were ductile, they tended to be welded together to form flat plates. After further milling and deformation, the flat pieces were work-hardened and then fractured to fragments. As shown in Fig. 3b, there were some fragments around the edge of the large plates. Because the malleability of the SnAgCu solder alloy was strong, the effect of cold welding was predominant compared to fracturing, especially when the particle size was reduced. Therefore, the large alloy ingots were produced.

Effect of Cu Concentration on Morphology of SnAgCu Solders

Morphologies of the SnAgCu MA powders with different Cu contents milled for 70 h are presented in Fig. 4. It is apparent that the slight variation of Cu composition has a strong effect on the morphology and size of the SnAgCu MA particle. The Sn3.5Ag0.2Cu powders after 70-h milling exhibited a strong cold-welding effect (Fig. 4a). Particles welded to larger ones during the MA process, and large alloy ingots formed with the diameter of 1 mm. Two types of morphologies are revealed in Fig. 4a, exhibiting the different stages of milling. Because solder powders were worn by the grinding mediums during the milling process, the surface would be more flat. The smoother surface shown in Fig. 4a was probably due to a more complete milling

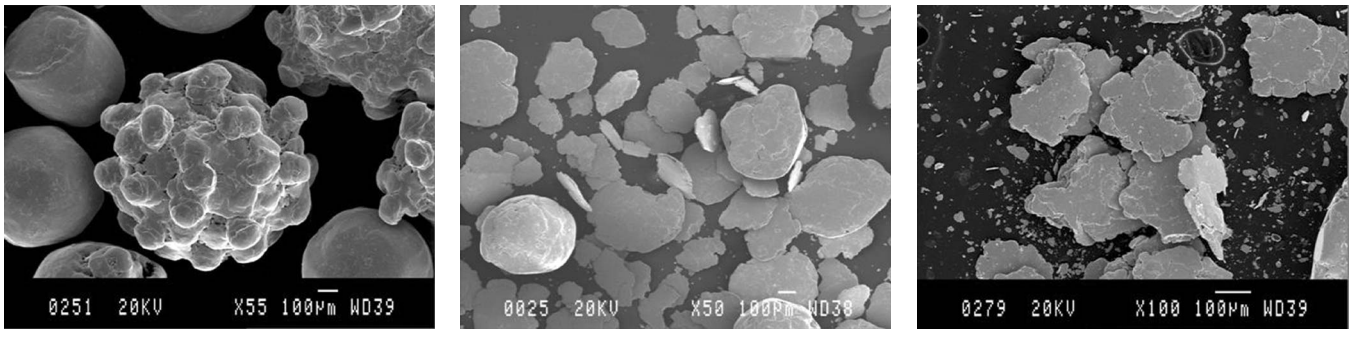

a b c

Fig. 4. The SEI micrographs of the Sn-3.5Ag-xCu MA powders milled for 70 h: (a) Sn3.5Ag0.2Cu, (b) Sn3.5Ag0.7Cu, and (c) Sn3.5Ag1Cu.

process. As compared to Fig. 3c, the surface of the solder alloy milled for 90 h became smoother.

When the Cu concentration increased slightly from 0.2–0.7 wt.% as in the case of Sn3.5Ag0.7Cu, the morphology changed from ingots to flat pieces (Fig. 4b). The size was less than 500 μm, smaller than that of Sn3.5Ag0.2Cu powders. As the Cu concentration further increased to 1 wt.%, the size distribution was bimodal (Fig. 4c). Thin, larger plates were surrounded by much smaller fragments. The small ones, around 10–50 μm, were cut from the edge of the thin plates. This means that the platelet Sn3.5Ag1Cu MA particle was work-hardened and tended to behave brittle.

Different types of mechanisms for the MA process have been proposed.[31,32] When the combination of materials for MA is ductile-ductile components, the ductile particles are flattened to platelet shapes and then cold-welded to form a composite lamellar structure of the constituent metals. If milling powder mixtures of ductile and brittle components, the ductile metal powder particles are flattened, while the brittle particles are fractured to small fragments, which will be trapped in the ductile particles. Those brittle particles trapped in the ductile particles play a very important role during milling because they would make the MA powders more brittle. Therefore, with further milling, the fracture effect will be predominant and size will be decreased. Recently, another lead-free solder material, SnAgBi, was prepared by the MA process.[28] When the brittle particle, Bi, was added into the ductile materials, including Sn and Ag, the size of the MA powder was decreased significantly from a few hundreds to nominally tens of micrometers. In this study, Sn, Ag, and Cu are rather ductile. Nevertheless, a different morphology was revealed for identical milling time. Powders with lower Cu composition, such as Sn3.5Ag0.2Cu, behaved like ductile-ductile materials. The welding phenomenon was evident. For powders with slightly higher Cu composition, such as Sn3.5Ag1Cu, they behaved like ductile-brittle materials. The work hardening, cutting, and fracturing were dominant. This means that some brittle phases might form in higher Cu-percent powder during the MA process, which, in turn, fractures the powders.

Distinct x-ray diffraction (XRD) peaks of Sn3.5Ag-xCu MA powders milled for 10 h were observed for different x values of the Cu concentration, as shown in Fig. 5. The Cu_6Sn_5 was formed when Cu concentration was as high as 0.7 wt.% in MA powders. However, only Sn peaks were observed in the XRD pattern if Cu concentration was as low as 0.2 wt.%. It should be noted that Cu_6Sn_5 appeared at the early stage of 10-h milling during the MA process, yet later disappeared at 70 h, as shown in Fig. 6. This is due to the fact that the ductile materials, such as Sn and Ag, would tend to disperse the Cu_6Sn_5 precipitation. As the milling process continued, they would be smeared outward and separated apart to an undetectable extent.

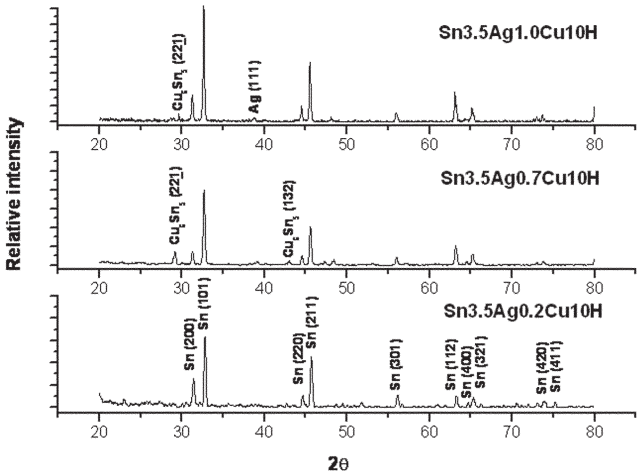

Fig. 5. The XRD peaks of Sn-3.5Ag-xCu powders milled for 10 h.

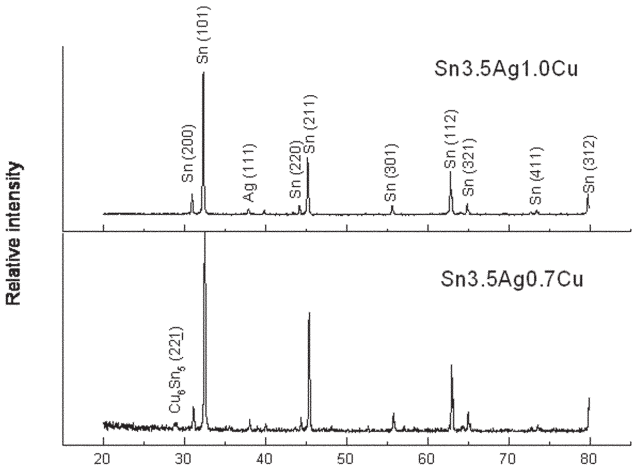

Fig. 6. The XRD peaks of Sn-3.5Ag-xCu powders milled for 70 h.

The result of XRD demonstrated the evidence of Cu_6Sn_5 formation during the MA process. In addition, the precipitation of Cu_6Sn_5 was also revealed in Fig. 7 by the SEM micrograph. There was slender precipitation dispersed on the flat surface of Sn3.5Ag0.7Cu. Although the phase was too fine to be detected in the EPMA, the presence of Cu_6Sn_5 should be ascertained with the aid of XRD results. As compared to Sn, Ag, and Cu, Cu_6Sn_5 behaved much more brittle. According to the milling mechanism of ductile-brittle materials as mentioned previously, brittle particles would cause MA powders to be fractured to smaller ones. Therefore, it is argued that brittle Cu_6Sn_5 should play an important role in the SnAgCu solder fabricated by the MA process.

Effect of Cu_6Sn_5 Doping on Morphology of SnAgCu Solders

To achieve the optimal milling condition of the MA process, various milling times were adopted in this study. Initially, the melting performance of the SnAgCu powder for short milling time was quite inferior because of the elevated melting point of the solder material. In practice, the melting temperature of

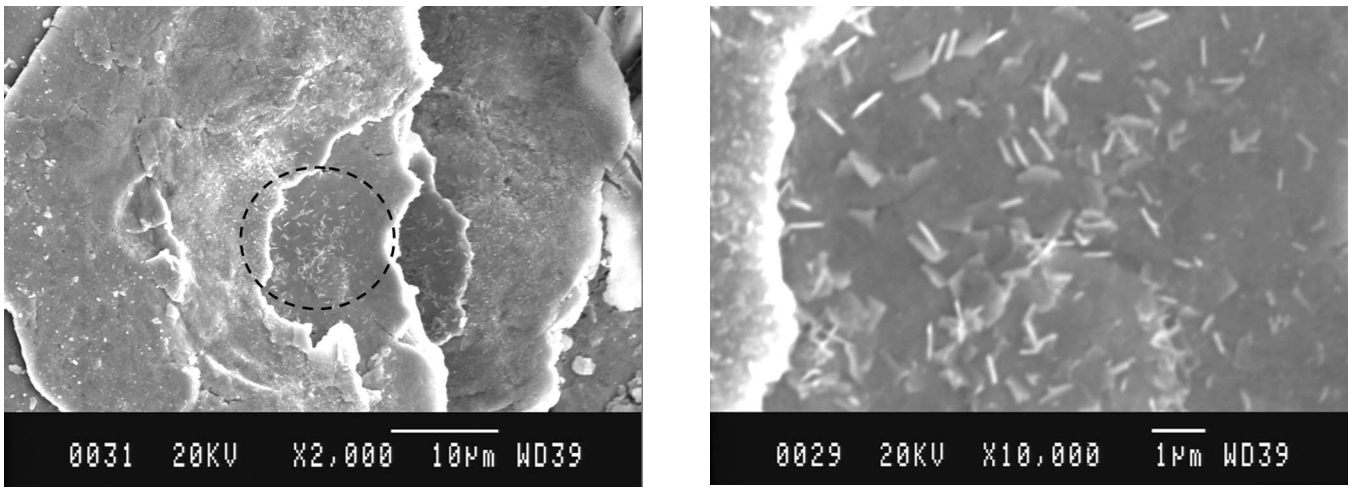

a b

Fig. 7. The SEI micrographs of the MA powders: (a) Sn-3.5Ag-0.7Cu milled for 10 h and (b) an enlarged view inside the circle in (a).

solders is a crucial parameter for the soldering process, which is the main factor in deciding the process temperature. The reason for the unusual melting point might be attributed to the incomplete milling and nonhomogeneous solder composition. It is argued that insufficient milling time could not provide sufficient free surfaces and other defects to enhance diffusion and alloying.[30] Longer milling time, up to 70 h, might ensure the complete milling.

The melting points of Sn3.5Ag0.2Cu MA powders milled for 70 h were measured to be 216°C on the basis of the DSC curves shown in Fig. 8. No other endothermic peak was found, indicating the complete melting of MA powders below 240°C reflow. The evaluated melting point shown in Fig. 8 was also very close to that of the eutectic SnAgCu solder alloy. Hence, the SnAgCu powders fabricated by the MA process in this study should be workable as commercial solder pastes during reflow.

However, the large size of the SnAgCu solder alloy fabricated by the MA process was not appropriate to today's solder bump technology. Therefore, the modification of the MA process to decrease the particle size was essential. As indicated previously, the particle size of the Sn3.5Ag1Cu solder alloy was reduced because of the formation of Cu_6Sn_5 during the MA process. In considering the milling mechanism for the combination of ductile-brittle materials by the MA process, the brittle particle, which dispersed in the ductile matrix, would make the MA powders more brittle. As a result, the MA particle would be fractured to a smaller size. Therefore, a further attempt was to add Cu_6Sn_5 powder into the solder powders to evaluate the effect of Cu_6Sn_5 on the MA process. Cu_6Sn_5 nano-powders less than 100 nm were produced by a chemical precipitation method, as shown in Fig. 9. The precipitate was single-phase Cu_6Sn_5 from the XRD, as indicated in Fig. 10. The Cu_6Sn_5, Sn and Ag were milled together by the MA process to form the Sn3.5Ag0.2Cu solder alloy.

After 70-h milling, the size of the Sn3.5Ag0.2Cu MA solder powder doped with Cu_6Sn_5 was obviously decreased to 20–100 μm, as shown in Fig. 11. The result of SEM demonstrated the fracturing effect of Cu_6Sn_5 on the SnAgCu solder alloy fabricated by the

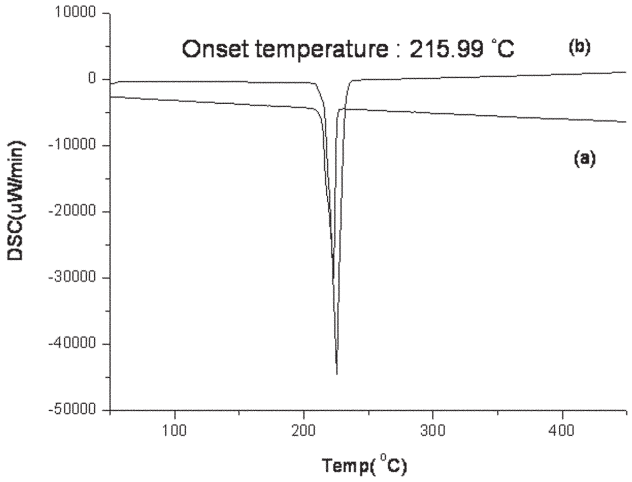

Fig. 8. The DSC profiles of Sn-3.5Ag-0.2Cu MA powders milled for 70 h: (a) doped with Cu_6Sn_5 nano-powder and (b) no doping.

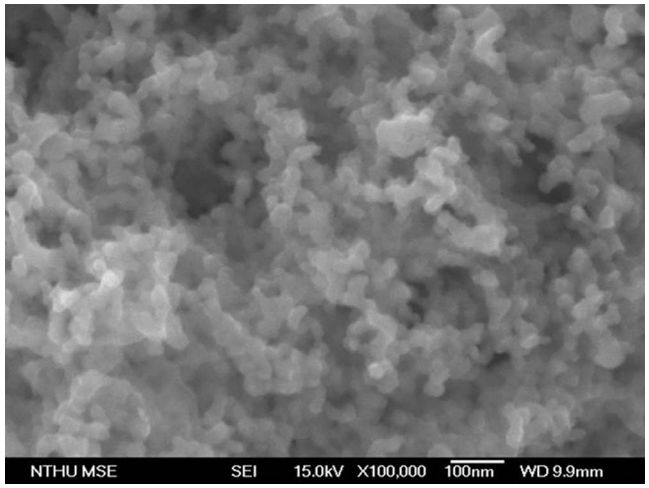

Fig. 9. The SEI micrographs of the Cu_6Sn_5 nano-powders.

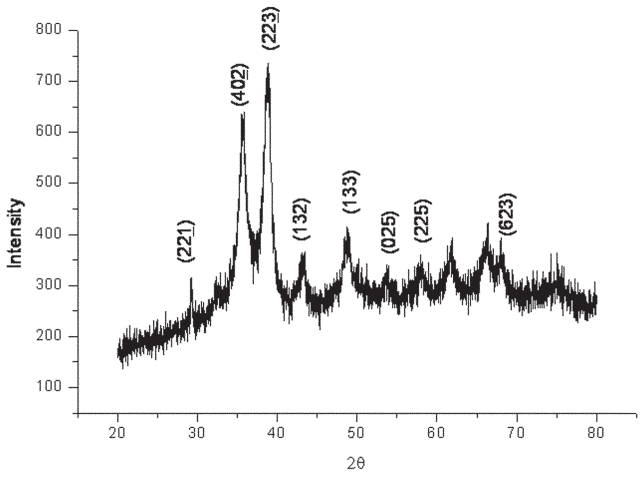

Fig. 10. The XRD peaks of the Cu_6Sn_5 nano-powders produced by the chemical method.

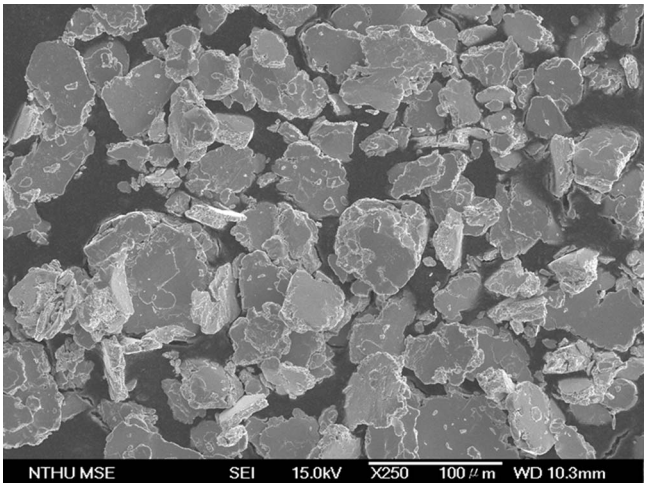

Fig. 11. The SEI of the Sn3.5Ag0.2Cu MA powders produced by milling Sn, Ag, and Cu_6Sn_5 nano-powders together for 70 h.

MA process. The milling mechanism of the ductile-brittle materials previously mentioned can be evidenced again. In addition, the melting point of the MA powders doped with Cu_6Sn_5 was also evaluated to be 215°C, which was identical to that of the MA powders fabricated without Cu_6Sn_5 doping (Fig. 8). Therefore, the Cu_6Sn_5-doped MA particle milled for 70 h not only ensured the appropriate melting point but also can be reduced to less than 100 μm in size to be applied on solder bump technology.

CONCLUSIONS

The SnAgCu solder alloy was successfully produced by the MA process with the composition of Cu in the solder alloy well controlled. During milling, Sn3.5Ag0.2Cu solder powders tended to be flattened and cold welded to form a large ingot at 70-h milling. However, Sn3.5Ag0.7Cu and Sn3.5Ag1.0Cu were fractured to small pieces for the same milling time because the brittle property of Cu_6Sn_5 precipitated in the high Cu-content solder alloy during the milling process. By doping nanosized Cu_6Sn_5 particles into original MA powders, the size of Sn-3.5Ag-0.2Cu would decrease significantly from 1 mm down to 10–100 μm. In addition, the melting point of Sn-Ag-Cu powders were reduced to 216°C, so that MA-derived powders could be employed as solder materials for the subsequent reflow process.

ACKNOWLEDGEMENTS

The financial support from the National Science Council, Taiwan, under Contract No. NSC- 92-2216-E-007-037, is acknowledged.

REFERENCES

1. M. Abtew and G. Selvaduray, *Mater. Sci. Eng. R: Rep.* 27, 95 (2000).
2. H. Reichl, A. Schubert, and M. Töpper, *Micro. Rel.* 40, 1243 (2000).
3. S. Topani, S. Gopakumar, P. Borgesen, and K. Srihari, *Annual Reliability Maintainability Symp.* (Piscataway, NJ: IEEE, 2002), pp. 423–428.
4. T.Y. Lee, W.J. Choi, K.N. Tu, J.W. Jang, S.M. Kuo, J.K. Lin, D.R. Frear, K. Zeng, and J.K. Kivilahti, *J. Mater. Res.* 17, 291 (2002).
5. D.R. Frear, J.W. Jang, J.K. Lin, and C. Zhang, *JOM* 53, 28 (2001).
6. W.H. Tao, C. Chen, C.E. Ho, W.T. Chen, and C.R. Kao, *Chem. Mater.* 13, 1051 (2001).
7. S.K. Kang et al., *Electronic Components and Technology Conf.* (Piscataway, NJ: IEEE, 2001), pp. 448–454.
8. S.K. Kang, H. Mavoori, S. Chada, C.R. Kao, and R.W. Smith, *J. Electron. Mater.* 30, 1049 (2001).
9. J.W. Jang, D.R. Frear, T.Y. Lee, and K.N. Tu, *J. Appl. Phys.* 88, 6359 (2000).
10. P.T. Vianco, S.N. Burchett, M.K. Neilsen, J.A. Rejent, and D.R. Frear, *J. Electron. Mater.* 28, 1290 (1999).
11. R.S. Rai, S.K. Kang, and S. Purushothaman, *Electronic Components and Technology Conf.* (Piscataway, NJ: IEEE, 1995), pp. 1197–1202.
12. L.L. Ye, Z. Lai, J. Liu, and A. Thölén, *Electronic Components and Technology Conf.* (Piscataway, NJ: IEEE, 2000), pp. 134–137.
13. M.E. Loomans and M.E. Fine, *Metall. Mater. Trans. A* 31A, 1155 (2000).
14. T.M. Korhonen, P. Su, S.J. Hong, M.A. Korhonen, and C.-Y. Li, *J. Electron. Mater.* 29, 1194 (2000).
15. J.R. Oliver, J. Liu, and Z. Lai, *Int. Symp. on Advanced Packaging Materials* (Reston, VA: IMAPS; Piscataway, NJ: IEEE, 2000), pp. 152–157.
16. W.R. Lewis, *Notes on Soldering* (Middlesex, England: Tin Research Institute, 1961), pp. 66–84.
17. J.W. Morris, Jr., J.L. Freer Goldstein, and Z. Mei, *JOM* 45, 25 (1993).
18. Y.Y. Chen, J.G. Duh, and B.S. Chiou, *J. Mater. Sci.: Mater. Electron.* 11, 279 (2000).
19. H.W. Miao and J.G. Duh, *Mater. Chem. Phys.* 71, 255 (2001).
20. H.W. Miao, J.G. Duh, and B.S. Chiou, *J. Mater. Sci.: Mater. Electron.* 11, 609 (2000).
21. Y.Y. Wei and J.G. Duh, *J. Mater. Sci.: Mater. Electron.* 9, 373 (1998), pp. 3–14.
22. S.L. Chen (M.S. thesis, National Tsing Hua University, Hsinchu, Taiwan, 1998).
23. T.Y. Lee, W.J. Choi, and K.N. Tu, *J. Mater. Res.* 17, 291 (2002).
24. C.E. Ho, R.Y. Tsai, Y.L. Lin, and C.R. Kao, *J. Electron. Mater.* 31, 584 (2002).
25. M.L. Huang, C.M.L. Wu, and J.K.L. Lai, *J. Mater. Sci.: Mater. Electron.* 11, 57 (2000).
26. C.M.L. Wu, M.L. Huang, J.K.L. Lai, and Y.C. Chan, *J. Electron. Mater.* 29, 1015 (2000).
27. M.L. Huang, C.M.L. Wu, J.K.L. Lai, and Y.C. Chan, *J. Electron. Mater.* 29, 1021 (2000).

28. H.L. Lai and J.G. Duh, *J. Electron. Mater.* 32, 215 (2003).
29. J. Wolfenstine, S. Campos, D. Foster, J. Read, and W.K. Behl, *J. Power Sources* 109, 230 (2002).
30. L. Lu, M.O. Lai, and S. Zhang, *J. Mater. Processing Technol.* 67, 100 (1997).
31. C. Suryanarayana, *Pro. Mater. Sci.* 46, 1 (2001).
32. J.S. Benjamin, *Sci. Am.* 234, 40 (1976).